



Effects of the growing-maize canopy and irrigation characteristics on the ability to funnel sprinkler water

ZHU Zhongrui^{1,2}, ZHU Delan^{1,2*}, GE Maosheng^{1,2}, LIU Changxin³

¹ College of Water Resources and Architectural Engineering, Northwest A&F University, Yangling 712100, China;

² Key Laboratory of Agricultural Soil and Water Engineering in Arid and Semiarid Areas, Ministry of Education, Northwest A&F University, Yangling 712100, China;

³ Breeding and Seed Production of Agricultural Crops of Tashkent State Agrarian University, Tashkent 100140, Uzbekistan

Abstract: Stemflow is vital for supplying water, fertilizer, and other crop essentials during sprinkler irrigation. Exploring the spatial and temporal variations of crop stemflow and its influencing factors will be essential to preventing soil water and nutrient ion's migration to deeper layers, developing, and optimizing effective sprinkler irrigation schedules. Based on the two-year experimental data, we analyzed the variation patterns (stemflow amount, depth, rate, and funneling ratio) of maize stemflow during the growing season, and clarified its vertical distribution pattern. Meanwhile, effects of sprinkler irrigation and maize morphological parameters on stemflow were investigated. The results showed that stemflow increased gradually as maize plant grew. Specifically, stemflow was small at the pre-jointing stage and reached the maximum at the late filling stage. The upper canopy generated more stemflow than the lower canopy until the flare opening stage. After the tasseling stage, the middle canopy generated more stemflow than the other positions. Variation in canopy closure at different positions was the main factor contributing to the above difference. As sprinkler intensity increased, stemflow also increased. However, the effect of droplet size on stemflow was inconsistent. Specifically, when sprinkler intensity was less than or equal to 10 mm/h, stemflow was generated with increasing droplet size. In contrast, if sprinkler intensity was greater than or equal to 20 mm/h, stemflow tended to decreased with increasing droplet size. Compared with other morphological parameters, canopy closure significantly affected the generation of stemflow. Funneling ratio was not significantly affected by plant morphology. Based on the results of different sprinkler intensities, we developed stemflow depth versus canopy closure and stemflow rate versus canopy closure power function regression models with a high predictive accuracy. The research findings will contribute to the understanding of the processes of stemflow involving the hydro-geochemical cycle of agro-ecosystems and the implementation of cropland management practices.

Keywords: sprinkler intensity; droplet diameter; morphological parameter; stemflow; spatial-temporal variation

Citation: ZHU Zhongrui, ZHU Delan, GE Maosheng, LIU Changxin. 2022. Effects of the growing-maize canopy and irrigation characteristics on the ability to funnel sprinkler water. *Journal of Arid Land*, 14(7): 787–810. <https://doi.org/10.1007/s40333-022-0022-z>

1 Introduction

Maize, a major food crop with high water consumption, occupied a huge planting area under cultivation, and its planting area is expanding worldwide (Hou et al., 2021). However, agricultural water is more limited than ever (Chen et al., 2020; Walczak, 2021). As a modern irrigation technology, sprinkler irrigation has played an irreplaceable role in agricultural water conservation,

*Corresponding author: ZHU Delan (E-mail: dlzhu@126.com)

Received 2022-02-25; revised 2022-06-01; accepted 2022-06-20

© Xinjiang Institute of Ecology and Geography, Chinese Academy of Sciences, Science Press and Springer-Verlag GmbH Germany, part of Springer Nature 2022

production increase, and agriproduct quality and efficiency improvement. Moreover, it is still being used widely (Chen et al., 2020; Zhu et al., 2021). In contrast to drip and surface irrigation, sprinkler water that falls through the plant canopy is partitioned into several parts. This water flows along with the sloping leaves or branches, and is channeled into the main stem, where it is concentrated at the stem base, and then infiltrates into the soil. Scientists have called this effective water as stemflow (Lamm and Manges, 2000; Zapata et al., 2018; Chen et al., 2021). In the agro-ecosystems, stemflow is an essential channel for irrigation water and nutrient input into the soil (Zheng et al., 2019). Scientists and field managers expect irrigation water and nutrients stored in the crop's main root layer. Compared with throughfall with a large infiltration area, stemflow is much like a localized point input of water and nutrients at the plant stem base. What's more, the excessive concentration of stemflow at the plant stem base induces incoming water to exceed infiltration (Herwitz et al., 1986). Several hydrogeological issues, such as runoff generation (Neave and Abrahams, 2002), soil erosion (Yin et al., 2020), groundwater recharge (Taniguchi et al., 2015), non-uniform distribution of soil moisture (Saffigna et al., 1976; Zapata et al., 2021; Zul Hilmi Saidin et al., 2021), nutrient ion loss, and transitional infiltration (Zul Hilmi Saidin et al., 2021) can also arise. For example, Glover and Gwynne (1962) found that soil moisture around maize plant stem base had already infiltrated 10 cm when the wetting depth at other positions was only a few millimeters. Furthermore, stemflow considerably contributes to the hydro-ecological and bio-geochemical cycles of the agro-ecosystems (Waiter and Price, 1988; Whitford et al., 1997; Levia and Frost, 2003; Carlyle-Moses et al., 2018). However, knowledge of crop stemflow during sprinkler irrigation is still deficient.

To avoid soil erosion and damage to crop leaf surfaces by sprinkler water droplets, sprinkler intensity and droplet diameter are the two key parameters to consider when selecting sprinkler heads or equipment, developing irrigation schedules, and guaranteeing irrigation efficiency (Zhang et al., 2017; Ge et al., 2018). Although numerous stemflow investigations have been carried out by scholars on the two parameters mentioned above, no consistent conclusions have been drawn. Zheng et al. (2018) found that maize plant stemflow amount and rate were positively correlated with rainfall amount and intensity. That is, the ability to generate stemflow was also enhanced with the higher rainfall amount and intensity. Ma et al. (2008b) also considered that high rainfall intensity positively affected maize plant stemflow yield. Similar findings have been found on woody trees (Zabret et al., 2018). However, Liu et al. (2015) concluded that the sprinkler water per unit area per unit time increased with increasing sprinkler intensity. The immense sprinkler amount tended to clog the pathways that transport stemflow on maize leaves, resulting in some stemflow converted into throughfall. Furthermore, similar negative correlations have been derived from research on soybean (Ma et al., 2008a). Therefore, they suggested that sprinkler intensity had a negative effect on the plant's ability to funnel irrigation water. The varied findings of previous studies have inspired us to continue exploring unknown horizons. On the other hand, because the larger diameter of droplets has higher kinetic energy than smaller ones, the plant leaves are significantly shaken and warped by the striking. Besides, many studies have only considered the effect of droplet size on canopy interception. For example, Kang et al. (2005) and Wang et al. (2020) found that plant canopy interception would decrease with increasing droplet diameter. They suggested that some intercepted water was converted into stemflow when the larger droplets impacted the leaves. However, there is a lack of necessary research on how water droplet size affects the plant's ability to generate stemflow. In addition, the motion of water droplets of different sizes on plant leaves varies considerably (Frasson and Krajewski, 2011). For example, the motion of small diameter droplets consists mainly of convergence and adhesion, whereas the motion of large diameter of droplets may include fragmentation and spattering. However, it is not known whether differences in motion impact the plant's ability to generate stemflow.

The influence of plant morphological characteristics on the partitioning of irrigation water cannot be neglected either (Tonello et al., 2021). Generally, previous studies have focused on the ability to generate stemflow using the maize canopy as a whole (Ma et al., 2008a, b; Liu et al.,

2015; Zheng et al., 2018). The maize leaves are spiraled on the stem, and the canopy is multi-layered in a vertical direction (Sher et al., 2018). Canopy structural parameters inevitably differ at different positions, and change with plant growth. However, the mechanism of the ability of maize canopy at different spatial positions to funnel sprinkler water or rainfall is unknown. In addition, Liu et al. (2015) and Zheng et al. (2018) analyzed the mechanism of leaf area index on the ability of maize canopy to generate stemflow, and predictive models for stemflow were developed using leaf area index as the independent variable. Ma et al. (2008b) also found that the ability to generate stemflow would increase with maize plant leaf area. In addition, in terms of funnel-like plant shape, Van Elewij (1989) set leaf height distance and leaf inclination as the primary control factors in developing a predictive model for stemflow. However, there are dozens of plant morphological parameters, and the empirical analysis of the effect of a single parameter on the plant's ability to generate stemflow is somewhat simplistic and ambiguous. If one morphological parameter chosen empirically is not a good representation of the whole plant, we would doubt the science and reliability of the predictive models developed for stemflow. Therefore, we still need to systematically evaluate the extent to which plant's morphological parameter influences the stemflow, and propose factors that can characterize the morphology of the whole plant.

If maize at the filling stage continue to receive sprinkler water from the same installation height at the jointing stage, this will inevitably affect the water distribution. Thus, the irrigator installation height based on crop growth is to meet practice requirements (Zhao et al., 2018). Fixing sprinkler installation height to the upper crop canopy can guarantee that the physical parameters of water striking the canopy at different growth stages are essentially the same. Maize leaves are broad and extensive compared with other plants. Therefore, we hypothesize that the capacity of maize canopy to generate stemflow increases gradually with increasing sprinkler intensity, and that the effect of sprinkler droplet size on the process of stemflow generation may not be significant. Therefore, the main aims of this study are: (1) to investigate the spatial and temporal variation in the ability of maize canopy to generate stemflow during the growing season; (2) to clarify the mechanisms by which irrigation features affect the generation of stemflow; (3) to comprehensively evaluate the influence of plant morphological parameters on stemflow, and attempt to obtain the factor that characterize the whole plant; and (4) to develop a highly representative and reliable model for predicting the generation of stemflow.

2 Materials and methods

2.1 Experimental design

Based on its high yield and large-scale use, we selected the maize variety Zhengdan 958 as the study material (Zheng et al., 2018). To follow a typical planting pattern, we sowed maize with plant spacing and row spacing of 30 and 60 cm, respectively, on 10 May, 2020, and 5 May, 2021. Because irrigation and fertilization were required at critical water demand periods, maize plants at the jointing, flare opening, tasseling, and filling stages were studied during the growing seasons in 2020 and 2021.

Sprinkler intensity and droplet diameter were set at three levels for each variable, and three replications were set for each group of treatments in the experiment. Previous studies have found that infiltration capacity of different soil types varies considerably, and that different soil types should correspond to different sprinkler intensities (Jin and Jiang, 1980; Wu, 1987). Irrigation needles with pore diameters of 0.70, 2.00, and 2.80 mm were selected to generate sprinkler water with three different droplet sizes. Three levels of sprinkler intensity were set at 10, 20, and 30 mm/h. Since the water output of different needles varied, sprinkler intensity was held constantly by changing the working pressure and the number of needles between trials. A total of nine treatments were included, abbreviated as follows: D_SI₁₀, D_SI₂₀, and D_SI₃₀ (small diameter water droplets at 10, 20, and 30 mm/h, respectively); D_MI₁₀, D_MI₂₀, and D_MI₃₀ (medium diameter water

droplets at 10, 20, and 30 mm/h, respectively); and D_{LI10} , D_{LI20} , and D_{LI30} (large diameter water droplets at 10, 20, and 30 mm/h, respectively). Maize growing in the field were cut with a blade and immediately placed on a bracket, and the cuts stems were sealed with paraffin wax. Due to the considerable variation in plant height across different growth stages and growing seasons, we set the height of needle outlet to 50 cm above the plants to ensure that the physical characteristics of droplets strikes were consistent in each test. To achieve complete saturation of the maize surface, we set the duration of sprinkler experiment to 1.0 h for each treatment, and the interval between each treatment was set to 0.5 h for smooth drainage of maize plant surface. In addition, the morphological parameters of plants were monitored at the beginning and end of each test to guarantee that no significant wilting of the plants occurred.

2.2 Experimental equipment

2.2.1 Sprinkler irrigation water droplets

The physical parameters of sprinkler water droplets include sprinkler intensity, diameter, velocity, and the landing angle of water droplets. If an off-the-shelf spray head or equipment was used for this experimental study, other parameters would change while sprinkler intensity was adjusted. This study would be meaningless if single-variable control could not be guaranteed. To achieve a single water tongue during sprinkler irrigation, we used a homemade panning sprinkler in this study. Its basic construction and spraying methods are shown in supplemental materials.

As shown in supplemental materials, the main structural parameters of the device include the following: a trolley moving speed of 0.034 m/s, a guide rail length of 5.00 m, a maximum extension height of the telescopic bracket of 4.50 m, a simulated sprinkler curtain width of 2.50 m, a fixed needle spacing of 0.05 m, and three types of orifice needles. YB150 instrument (Xi'an Instrument Factory, China) with a range of 0.40 MPa (precision of 0.01 MPa) was used for pressure gauge. The device works as follows: the power supply provides power for the variable-rate pump and the mobile trolley, and the working pressure of the needles for water droplet generation is controlled by adjusting the speed of the variable-rate pump. A pressure gauge displays the actual working pressure of the needle. The variable-rate pump retrieves water from a reservoir, and the water flows through a hose to the needles. A single aluminum alloy pipe with several fixed needles is mounted on a height-adjustable telescopic bracket, and fixed to a variable-speed mobile cart. Automatic steering devices are installed at both ends of the cart. The single sprinkler water curtain can then be sprayed in cycles above the crop canopy. It was essential to highlight that the height of the aluminum water pipeline installed with needles was adjustable as maize plant grew.

The equipment was multi-functional. It can adjust the sprinkler intensity, diameter, and velocity of water droplets, and change the landing angle. As shown in supplemental materials, this study placed the needle vertically to achieve the scattering of sprinkler droplets, and the sprinkler water could be sprayed upward. The vertical falling of sprinkler water droplets could avoid the effect of landing angle on the ability of crop canopy to funnel sprinkler water because our previous work showed that the chance of their contact with corn canopy would be greater with the smaller landing angle (Zhu et al., 2021, 2022). In addition, three-needle diameters (0.70, 2.00, and 2.80 mm) were tested to regulate droplet diameter.

As shown in supplemental materials (Figs. S1–S4), the diameter of droplets increased with increasing needle gauge size. Moreover, the normal working conditions based on upward spraying ultimately met the requirements of sprinkler irrigation with water droplets sufficiently scattered.

2.2.2 Spatial arrangement of maize plant and stemflow collector

We placed the tested plants on a movable bracket at 50 cm above the ground according to the plant distribution in the field. The bracket was arranged with adjustable spacing crossbars. Each crossbar was welded with 15 cm iron nails, and spaced 10 cm apart. Figure 1a showed the spatial arrangement of maize plant and micro-scale spatial scope created, and Figure 1b showed the arrangement of stemflow collectors. Sixteen maize plants with insignificant differences in

morphological parameters were selected from the field. Four plants were used to create a micro-scale spatial extent, and the rest were used as protective rows. This study collected stemflow of four maize plants on a micro-scale spatial scope using the homemade device (Fig. 1b).

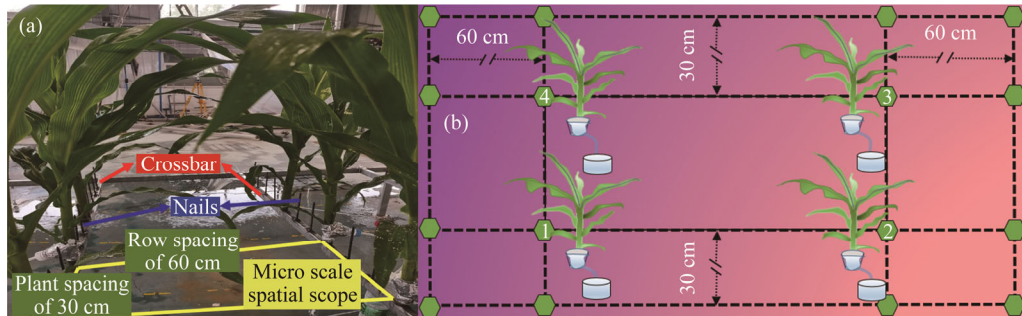


Fig. 1 Arrangement of maize plant (a) and stemflow collection device (b) in the experiment

2.3 Stemflow

2.3.1 Stemflow collection and calculation

As an essential independent variable in this study, it was necessary to calibrate sprinkler intensity for different treatments by adjusting the working pressure and changing the number of needles in each treatment to ensure the same sprinkler intensity for different growth stages of the plants. Sprinkler water was collected using three row catchment boxes. The average water collected across all catchment boxes was designated as the water volume. Because the opening area of each collector box was 100 cm², the sprinkler water volume in weight-based units (g) was converted to water volume in depth-based unit (G , mm).

Stemflow was collected from four maize plants in the micro-scale spatial extent using a homemade device consisting of a funnel mounted on the maize stem base, a drainage pipe, and a container. The funnel surrounded the maize stem base, and the gap was sealed to prevent stemflow from leaking. The two ends of the drainage pipe were connected to the bottom of the funnel and the top of the container, and the drainage pipe transported stemflow from the funnel to the container (Fig. 2).

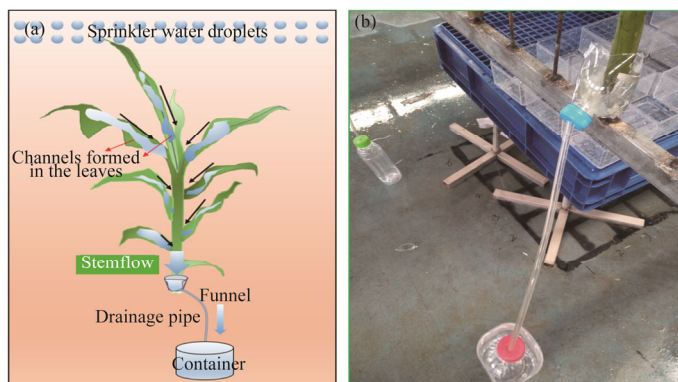


Fig. 2 Schematic diagram of the stemflow generation process (a) and collection device (b)

Stemflow collected from four maize plants was weighed when the water stopped dripping from the collection device. Stemflow amount generated by each plant was averaged. Equivalent water depth for stemflow was calculated, as shown in Equation 1:

$$S_d = \frac{S}{A} \times 10, \quad (1)$$

where S is the average stemflow mass (g); S_d is the stemflow depth (mm); and A is the average

surface area of each maize plant (cm^2 , $30 \text{ cm} \times 60 \text{ cm}$).

Stemflow rate (SR, %) was calculated as the ratio of stemflow amount to sprinkler water volume (G) as shown in Equation 2.

$$\text{SR} = \frac{S}{G} \times 100\%. \quad (2)$$

In addition, the leaves and branches within the plant canopy are at an angle to the horizontal, and the overall shape of the plant canopy looks like a funnel. To evaluate the ability of a specific plant canopy to funnel sprinkler water or rainfall, scientists have introduced the funneling ratio (FR, dimensionless). If FR is greater than 1, the plant's canopy structure is conducive to generate stemflow (Herwitz, 1986; Carlyle-Moses, 2018).

$$\text{FR} = \frac{S}{\text{BA} \times G}, \quad (3)$$

where FR is the funneling ratio of maize plant (dimensionless); and BA is the basal area of maize stem (cm^2).

2.3.2 Vertical distribution of the ability of maize canopy to funnel sprinkler water

The number of maize leaves varies considerably at different growth stages. For example, the number of leaves at the jointing stage may only be 4 or 5, while the number after the tasseling stage will reach 12 or more. Therefore, to investigate the ability of maize canopies at different spatial positions to funnel sprinkler water, we divided the whole canopy into upper and lower layers, i.e., two treatments during the jointing and flare opening stages. According to the plant growth, we divided the whole canopy into three layers, i.e., upper, middle, and lower layers, at the tasseling and filling stages (Fig. 3). In addition, because this section only involved the change of canopy structure, we selected the sprinkler working conditions for DM_{120} . Three replicated sprinkler experiments were set up for each of the above treatments. Please refer to Sections 2.2.2 and 2.3.1 for the set-up and calculation of other parameters and indicators during the test. It is essential to highlighting that the layered treatments were for four maize plants forming the micro-scale spatial scope and not for a single maize plant alone.

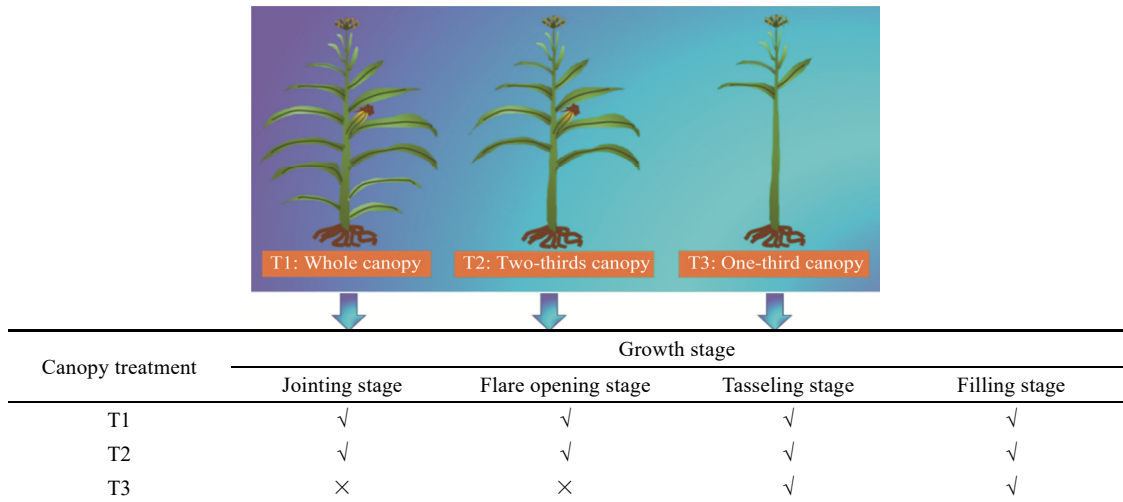


Fig. 3 Vertical layering of maize canopy across the micro-scale spatial scope

2.4 Sprinkler irrigation

The uniformity of sprinkler water distribution over the moving range of sprinkler unit was evaluated using the Christiansen uniformity coefficient (CU) in this study.

$$\text{CU} = \left(1 - \frac{\sum_{i=1}^n |h_i - \bar{h}|}{n\bar{h}} \right) \times 100\%, \quad (4)$$

where CU is the Christiansen uniformity coefficient (%); n is the number of measurement points; h_i is the sprinkler water depth collected at the i^{th} measurement point (mm); and \bar{h} is the average of the sprinkler water depth at all measurement points (mm).

Each test calibrated sprinkler intensity with irrigation height fixed at 50 cm above the plants. Water droplets were released in a nearly vertical upward flight path. Therefore, we could assume that sprinkler droplets' physical parameters or characteristics when striking the canopy at different growth stages under different treatments were constant. The diameter and velocity of individual water droplet were recorded using a two-dimensional video distrometer (2DVD), and the operating principle can be found in the relevant researches (Ge et al., 2018; Chen et al., 2020).

Total kinetic energy of the sprinkler water was calculated using the following equation:

$$Ke_{\text{Total}} = \sum_{i=1}^n \frac{1}{12} \pi \times d_i^3 \times \rho_w \times v_i^2, \quad (5)$$

where Ke_{Total} is the total kinetic energy (J); i is the number of water droplets; d_i is the diameter of the i^{th} water droplet (mm); ρ_w is the density of water (kg/m^3); and v_i is the velocity of the i^{th} water droplet (m/s).

Kinetic energy per unit volume of sprinkler water (Ke_v , $\text{J}/(\text{m}^3 \cdot \text{mm})$) was calculated using the following equation:

$$Ke_v = \frac{Ke_{\text{Total}}}{1000 \sum_{i=1}^n \frac{1}{6} \times \pi \times d_i^3}. \quad (6)$$

The formula for calculating the kinetic energy intensity of sprinkler water was as follows:

$$SP = Ke_v \frac{P}{3600}, \quad (7)$$

where SP is the kinetic energy intensity ($\text{J}/(\text{m}^2 \cdot \text{s})$); and P is the sprinkler intensity (mm/h).

The drop size distribution (DSD) of droplets was described using the relative volume of droplets (volume ratio, dimensionless), and the volume percentage of droplets in each diameter range ($V(D_j)$) was calculated using the following equation (Levia et al., 2017):

$$V(D_j) = \frac{\sum_i^{N_j} V_i}{V_{\text{Total}}}, \quad (8)$$

where i is the i^{th} droplet within the sprinkler water droplet group; j is the j^{th} diameter classification; N_j is the number of droplets within the j^{th} droplet diameter classification; V_i is the volume of the i^{th} droplet within the water droplet group (mm); and V_{Total} is the total volume of the water droplet population (mm). The range of each droplet diameter was set to 0.50 mm.

The diameter of water droplets was calculated by the method of Levia et al. (2017). In order to compare and analyze the difference in water droplet diameters at different sprinkler intensities with the same needle gauge, we calculated the three characteristic values (D_{25} , D_{50} , and D_{75}) of droplet diameter.

2.5 Morphological parameters of maize

Each parameter of four maize plants constituting micro-scale spatial scope was calculated. The leaf surface area of maize (LSA, cm^2) was calculated as follows:

$$\text{LSA} = \sum_{i=1}^n k \times L_i \times W_i, \quad (9)$$

where n is the number of maize leaves; k is the correction coefficient for leaf area (0.75); L_i is the length of the i^{th} leaf (cm); and W_i is the maximum width of the i^{th} leaf (cm).

In contrast to previous calculation methods, LSA per unit of ground area within the canopy of a broadleaf plant was regarded as leaf area index (LAI) of that plant, which was calculated by the following equation (Zheng et al., 2018).

$$LAI = \frac{LSA \times N}{10000}, \quad (10)$$

where LAI is the leaf area index (m^2/m^2); and N is the number of maize plant per square meter of soil surface area.

In this study, maize cob was considered an ellipsoid with a circular section, but only half of the cob surface had a positive effect on the stemflow generation. Therefore, the formula for calculating the cob surface area (CSA, cm^2) can be referred to as the formula for calculating the ellipsoid surface area, except that its value was half of the magnitude of ellipsoid surface area. In addition, the sprinkler water droplets fall approximately vertically, and the contact area of water droplet with the stem and the inflorescence is very limited. The stem and inflorescence surface area has a negligible effect on the stemflow amount. Therefore, the formula used in this paper to calculate the plant's effective surface area (PESA) was shown below:

$$PESA = LSA + CSA. \quad (11)$$

The following morphological parameters of maize were measured. The diameter of cut stem was considered as stem diameter (SD, cm). Plant height (PH, cm) was the distance between the highest point of each plant and the ground. Canopy thickness (CT, cm) was the distance between the highest and the lowest points of leaves. Canopy closure (CC, %) was measured and displayed using the Canopeo software installed on a mobile phone (Patrignani and Ochsner, 2015). leaf height distance (LHD, cm) was the average of horizontal distance between the highest point of the leaf and the stem. Leaf height distance of larger leaves (LHDLL, cm) was the average horizontal distance between the highest point of a leaf with a larger shaded area and the stem. Leaf inclination (LI, °) was the angle between the central leaf vein and the horizontal plane, as measured using a protractor. The leaf inclination of each maize plant was taken as the average for all the leaves. The leaf inclination of larger leaves (LILL, °) was the average angle between the central veins and the horizontal plane of a leaf with a larger shaded area. Plant fresh weight (PFW, g) was measured using the weighing method, and included the fresh weight of leaves (FLW, g), stems (FSW, g), cobs (FCW, g), and male and female inflorescences (FWI, g). In addition, we measured the dry weight of the plants (PDW, g), leaves (LDW, g), stems (SDW, g), cobs (CDW, g), and male and female inflorescences (IDW, g) using the method of Li et al. (2016).

2.6 Statistical analysis

We used a one-way analysis of variance ($P < 0.05$) to test the statistical differences in the ability to funnel sprinkler water at different growth stages of maize. The Pearson's coefficient was used to analyze the correlation between plant morphological parameters and ability to funnel sprinkler water. Significant differences between different growth stages and between different treatments were determined using t -test ($P < 0.05$). In addition, we used Pearson's coefficient to analyze the correlations between different morphological parameters, and obtain a morphological parameter representative of whole maize plant. We developed power function prediction models of representative morphological parameter with stemflow amount and rate using two-thirds of the experimental data based on different sprinkler intensities and droplet diameters. The remaining experimental data were used to validate the accuracy of models. The determination coefficient (R^2), root mean square error (RMSE), and standard root mean square error (NRMSE) were used to evaluate the accuracy of each developed predictive model (Yang et al., 2014). High R^2 and low RMSE and NRMSE values indicated the accuracy and generalization capability of the prediction model. All descriptive statistical analyses and regressions were performed using SPSS v.16.0 statistical software (SPSS Inc., USA), and all data figures were created using Sigmaplot v.10.0 (Systat Software, San Jose, USA).

3 Results

3.1 Stability of the sprinkler irrigation equipment

In order to achieve the same sprinkler intensity with different needle orifices, we regulated the

sprinkler intensity by adjusting the working pressure and number of needles to stabilize it in the desired value range. As shown in Table 1, the actual intensity ranged between 9.68–11.31, 19.86–20.98, and 29.46–32.49 mm/h for 10, 20, and 30 mm/h sprinkler intensity levels, respectively. The percentage ranges between actual and theoretical values were 96.80%–113.10%, 99.30%–104.90%, and 98.20%–108.30%, respectively. In addition, D_{50} of sprinkler water droplets generated by small, medium and large needles ranged between 1.48–1.49, 3.65–3.69, and 7.08–7.13 mm, respectively. Moreover, as supplemental materials shown, DSDs for different intensities generated by the same orifice needle had similar distribution trends, and the corresponding D_{25} , D_{50} and D_{75} showed similarity. What's more, taking D_{50} as an example, supplemental materials exhibited the spatial distribution of sprinkler water corresponding to this treatment. As shown in supplemental materials, the distribution of sprinkler water in the direction vertical to the guide rail was very uniform, and the sprinkler water in the direction of cart movement also had a similar distribution pattern. The other treatments also had such a high uniformity coefficient of sprinkler water distribution ($CU > 85\%$). The above results showed that droplet diameters at different sprinkler intensities generated under the same needle gauge had good uniformity and stability. It was possible to manage the constant value of sprinkler intensity by appropriately changing the working pressure and the number of needles.

Table 1 Physical characteristics of sprinkler water droplets

Different treatments			Actual sprinkler intensity (mm/h)	CU (%)	Ke_{Total} (J)	Ke_v (J/(m ² ·mm))	SP (J/(m ² ·s))	Droplet diameter (mm)		
Droplet size	Sprinkler intensity (mm/h)	Abbre- viation						D_{25}	D_{50}	D_{75}
Small diameter	10	$D_{SI_{10}}$	9.68±0.13	96.12	0.25±0.08	3.59±0.71	0.010±0.001	0.86±0.13	1.48±0.26	1.96±0.39
	20	$D_{SI_{20}}$	20.17±2.01	95.16	0.56±0.11	4.99±0.53	0.028±0.005	0.79±0.09	1.49±0.19	1.99±0.44
	30	$D_{SI_{30}}$	29.46±1.98	93.84	0.98±0.09	6.16±1.02	0.050±0.007	0.82±0.21	1.48±0.43	1.93±0.26
Medium diameter	10	$D_{MI_{10}}$	10.24±0.98	95.59	1.05±0.14	4.70±0.95	0.013±0.002	2.76±0.68	3.68±0.65	3.96±0.47
	20	$D_{MI_{20}}$	19.86±1.59	93.48	1.61±0.25	6.12±0.57	0.034±0.008	2.83±0.79	3.65±0.49	3.98±0.88
	30	$D_{MI_{30}}$	30.86±2.47	94.57	3.06±0.63	7.60±1.06	0.065±0.009	2.79±0.93	3.69±0.55	3.99±0.75
Large diameter	10	$D_{LI_{10}}$	11.31±2.02	93.41	1.59±0.23	8.13±0.99	0.026±0.005	6.65±1.59	7.11±0.98	7.86±1.12
	20	$D_{LI_{20}}$	20.98±1.95	92.49	2.85±0.42	10.69±1.48	0.062±0.004	6.63±1.43	7.13±1.95	7.91±0.98
	30	$D_{LI_{30}}$	32.49±2.69	89.19	4.69±0.18	11.49±0.95	0.104±0.008	6.51±1.79	7.08±1.36	7.88±1.25

Note: CU, Christensen uniformity coefficient; Ke_{Total} , total kinetic energy; Ke_v , kinetic energy per unit volume; SP, kinetic energy intensity. Mean±SD.

3.2 Variation in the ability of maize plant to funnel sprinkler water

3.2.1 Effects of maize canopies at different growth stages

To investigate how the ability of maize plant to funnel sprinkler water varies throughout the growing season, we statistically analyzed the variations of the ability to generate stemflow at different growth stages. The results revealed that, based on plant growth and evolutionary process, their variation ranges (averages) of stemflow amount at the jointing stage, flare opening stage, tasseling stage, and filling stage were 135.00–714.60 (326.00), 216.00–1400.40 (881.40), 414.00–2269.80 (1381.80), and 433.80–2381.40 (1422.30) mL, respectively (Fig. 4a). For stemflow depth, their variation ranges (averages) at different growth stages were 0.75–5.01 (2.61), 1.20–8.82 (4.90), 2.30–13.14 (7.68), and 2.41–13.45 (7.90) mm, respectively (Fig. 4b). For stemflow rate, their variation ranges (averages) at different growth stages were 2.89%–17.24% (9.05%), 5.19%–37.14% (22.26%), 8.93%–62.51% (35.19%), and 9.78%–63.40% (36.29%), respectively (Fig. 4c). In addition, for stemflow ratio, their variation ranges (averages) at different growth stages were 8.71–137.04 (63.87), 14.06–100.52 (62.22), 19.99–139.95 (83.68), and 20.58–133.46 (81.34), respectively (Fig. 4d). The present results showed that stemflow amount, stemflow depth, stemflow rate, and funneling ratio all increased with the growth of maize plant, and most of parameters reached their maximum values at the latest stage. In addition, significant

differences ($P<0.05$) between the stemflow parameters of maize plant at different growth stages within a given growing season was found.

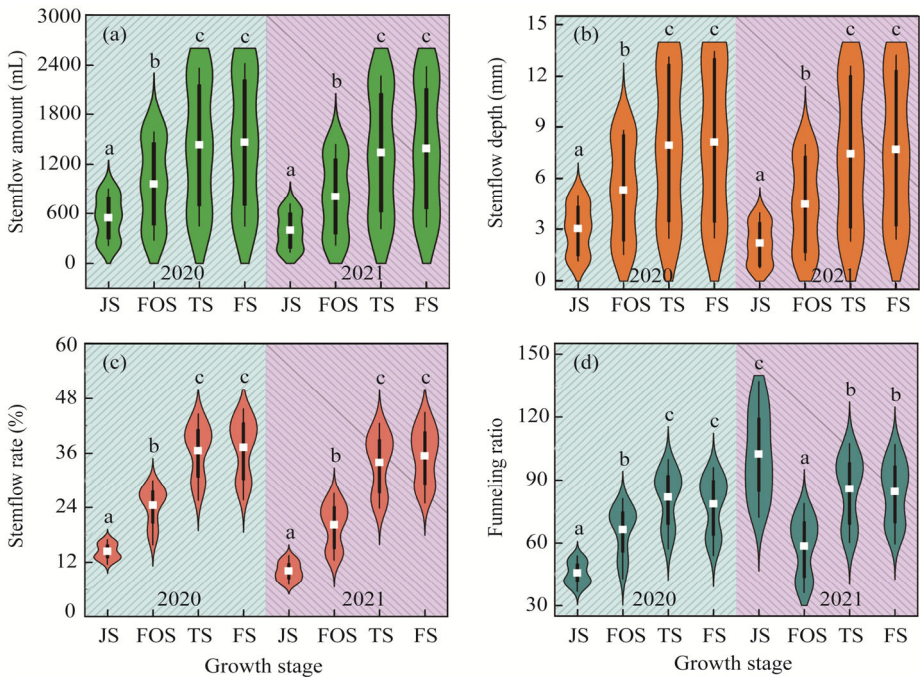


Fig. 4 Maize stemflow parameters at different growth stages in 2020 and 2021. (a), stemflow amount; (b), stemflow depth; (c), stemflow rate; (d), funneling ratio. JS, jointing stage; FOS, flare opening stage; TS, tasseling stage; FS, filling stage. Different lowercase letters indicate significant differences among different growth stages within the same year at $P<0.05$ level.

3.2.2 Effect of maize canopy at different positions

As shown in Figure 5, the values of the upper and lower canopies to generate stemflow at the jointing stage was 74.32% and 25.68%, while the corresponding values at the flare opening stage were 62.88% and 37.12%, respectively. After the flare opening stage, the maize canopy was divided into the upper, middle, and lower layers at the tasseling and filling stages. The ability of the upper, middle, and lower canopies to generate stemflow at the tasseling stage was 21.70%, 68.72%, and 9.58%, and the corresponding values at the filling stage were 21.01%, 71.46%, and 7.53%, respectively.

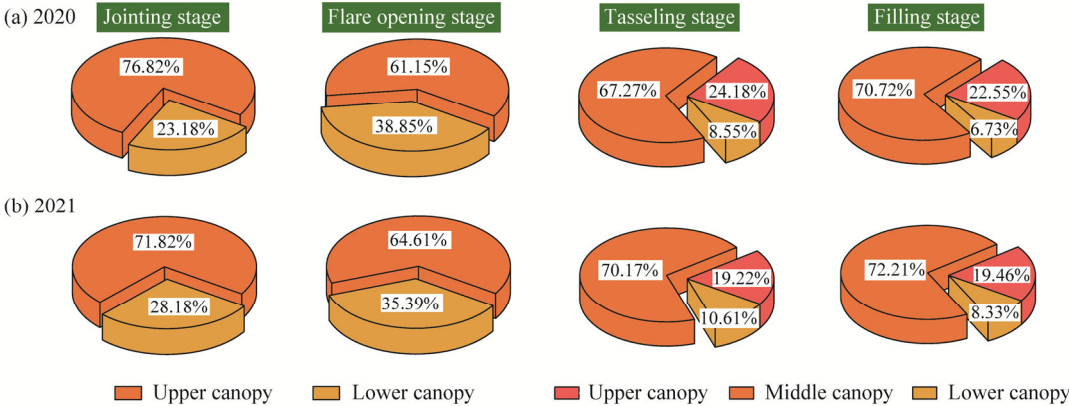


Fig. 5 Effects of maize canopies at different positions and growth stages on stemflow in 2020 (a) and 2021 (b)

3.3 Effects of irrigation characteristics on maize stemflow

The stemflow amounts (averages) with the 10, 20, and 30 mm/h sprinkler intensity were 135.00–635.00 (390.08), 333.00–1546.00 (1031.55), and 576.00–2421.00 (1694.70) mL, respectively (Fig. 6a and b). The stemflow depths (averages) were 0.75–3.53 (2.17), 1.85–8.59 (5.73), and 3.20–13.45 (9.42) mm, respectively (Fig. 6c and d). Moreover, the stemflow rate (averages) were 7.07%–31.21% (20.76%), 9.06%–42.59% (28.20%), and 9.85%–45.66% (30.50%), respectively (Fig. 6e and f). In addition, the funneling ratios were 59.03, 80.13, and

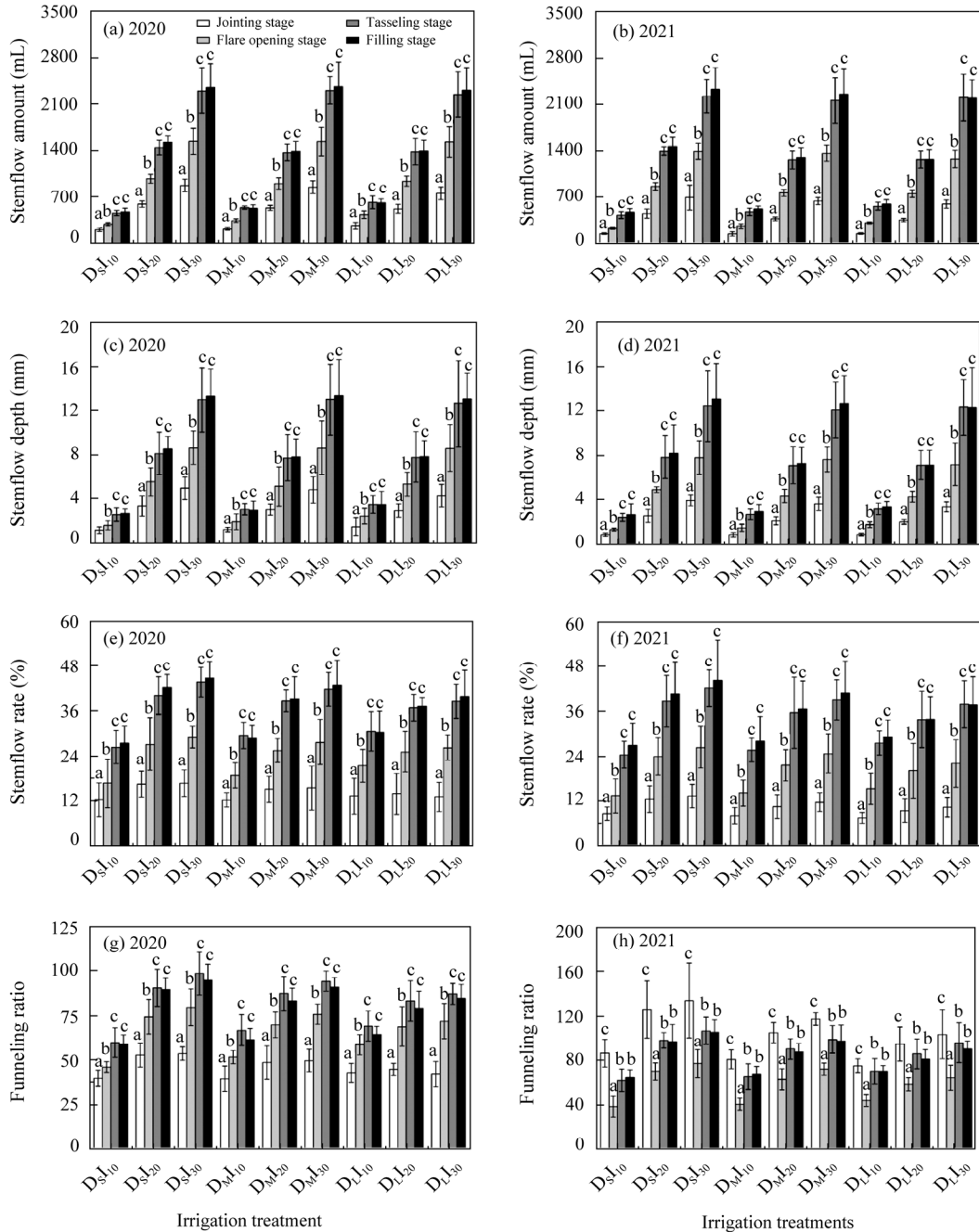


Fig. 6 Effects of irrigation characteristics on maize stemflow in 2020 and 2021. (a and b), stemflow amount; (c and d), stemflow depth; (e and f), stemflow rate; (g and h), funneling ratio. Different lowercase letters within the same treatment indicate significant differences at $P < 0.05$ level. The detailed treatments can be found in Table 1.

86.69, respectively (Fig. 6g and h). As sprinkler intensity increased by each magnitude or level, stemflow amount and depth also increased in response, while stemflow rate and funneling ratio did not exhibit the same trend. Specifically, if sprinkler intensity increased from 10 to 20 mm/h, the stemflow rate and funneling ratio increased by 7.44% and 21.10, respectively. When sprinkler intensity increased from 20 to 30 mm/h, the stemflow rate and funneling ratio increased by only 2.30% and 6.56, respectively. The different trends indicated that four parameters did not respond to increasing sprinkler intensity with the same mechanism.

In this study, the regulation of droplet sizes was achieved by using three orifice needles, which were selected optimally in advance. Moreover, the droplet sizes produced by the same orifice with different sprinkler intensities were very similar (Table 1). Therefore, we used the average method (D_{50}) to calculate the droplet sizes of sprinkler droplets generated by different orifice sizes, and the average value was the droplet diameter corresponding to that type of needle. The results indicated that when the needle apertures were 0.70, 2.00, and 2.80 mm, the corresponding sprinkler droplet diameters were 1.48, 3.67, and 7.11 mm, respectively. Generally, when the droplet diameters were 1.48, 3.67, and 7.11 mm, the corresponding ranges (averages) of stemflow amount were 135.00–2421.00 (1033.00), 144.00–2363.40 (1032.00), and 138.60–2421.00 (999.15) mL, respectively. The corresponding ranges (averages) of stemflow depth were 0.75–13.45 (5.87), 0.80–13.13 (5.74), and 0.77–13.45 (5.70) mm, respectively. In addition, the ranges (averages) of stemflow rate were 7.75%–45.66% (27.51%), 7.52%–43.58% (26.42%), and 7.07%–40.41% (25.54%), respectively. The corresponding ranges (averages) of funneling ratio were 8.71–137.04 (116.50), 8.83–119.29 (72.94), and 40.97–106.42 (71.82), respectively. The experimental data showed the stemflow rate (Fig. 6a and b), depth (Fig. 6c and d), rate (Fig. 6e and f), and funneling ratio (Fig. 6g and h) decreased significantly as the droplet diameter decreased.

3.4 Effects of morphological parameters

As shown in Table 2, when excluding the morphological parameters related to leaf height distance and leaf inclination, we found that stemflow amount, depth, and rate showed significant positive correlations with the remaining seven morphological parameters ($R^2 > 0.80$, $P < 0.01$). Besides, the effect of canopy closure on stemflow generation was more significant than other morphological parameters ($R^2 = 0.982$, $P < 0.01$). For example, if canopy closure increased from 20.15% to 93.18%, stemflow amount increased from 393.60 to 1459.40 mL, stemflow depth increased from 2.19 to 8.11 mm, and stemflow rate increased from 10.06% to 37.23%. Furthermore, none of the eleven selected morphological parameters had a good correlation with funneling ratio in this study, and only the leaf height distance and leaf inclination showed a weak correlation with funneling ratio ($0.300 < R^2 < 0.800$, $P > 0.05$).

3.5 Identification of main control factor

As shown in Figure 7, the Pearson's correlation coefficients between canopy closure and maize morphological parameters were greater than those of other morphological parameters ($0.424 < R^2 < 0.989$). The correlation coefficients between different morphological parameters indicated the degree to which the two could be substituted for each other. In other words, excluding some uncontrollable factors, canopy closure better characterized the morphological characteristics of whole maize plant. In addition, canopy closure significantly affected the ability of maize plants to generate stemflow (Table 2; $P < 0.01$). Therefore, the present findings indicated that canopy closure would need to be set as the primary control factor when developing a stemflow prediction model.

3.6 Prediction model of stemflow

Based on different sprinkler intensities, droplet diameters, and two-thirds of all trial data randomly selected during two growing seasons, power function models of canopy closure versus stemflow depth and stemflow rate were obtained using regression analysis (Table 3). The data in Table 3 showed that the predictive models for stemflow depth and stemflow rate based on different sprinkler intensities had good validity ($R^2 > 0.80$, $P < 0.05$) compared with droplet size

Table 2 Correlation between stemflow and plant morphological parameters

Plant morphological parameter	Statistical result	Streamflow variable			
		<i>S</i>	<i>S_d</i>	SR	FR
LAI	<i>R</i> ²	0.959	0.959	0.959	−0.048
	<i>P</i>	<0.01	<0.01	<0.01	>0.05
CC	<i>R</i> ²	0.982	0.982	0.982	0.074
	<i>P</i>	<0.01	<0.01	<0.01	>0.05
PH	<i>R</i> ²	0.951	0.951	0.948	0.084
	<i>P</i>	<0.01	<0.01	<0.01	>0.05
CT	<i>R</i> ²	0.933	0.933	0.93	0.045
	<i>P</i>	<0.01	<0.01	<0.01	>0.05
SD	<i>R</i> ²	0.839	0.839	0.841	−0.339
	<i>P</i>	<0.01	<0.01	<0.01	>0.05
LHD	<i>R</i> ²	0.368	0.368	0.376	−0.628
	<i>P</i>	>0.05	>0.05	>0.05	>0.05
LHDLL	<i>R</i> ²	0.847	0.847	0.852	−0.264
	<i>P</i>	<0.01	<0.01	<0.01	>0.05
LI	<i>R</i> ²	0.479	0.479	0.477	0.503
	<i>P</i>	>0.05	>0.05	>0.05	>0.05
LILL	<i>R</i> ²	−0.955	−0.955	−0.954	−0.357
	<i>P</i>	<0.01	<0.01	<0.01	>0.05
PEW	<i>R</i> ²	0.961	0.961	0.962	0.219
	<i>P</i>	<0.01	<0.01	<0.01	>0.05
PDW	<i>R</i> ²	0.847	0.847	0.850	0.234
	<i>P</i>	<0.01	<0.01	<0.01	>0.05

Note: LAI, leaf area index; CC, canopy closure; PH, plant height; CT, canopy thickness; SD, stem diameter; LHD, leaf height distance; LHDLL, leaf height distance of the larger leaves; LI, leaf inclination; LILL, leaf inclination of the larger leaves; PFW, plant fresh weight; PDW, plant dry weight. *S*, stemflow amount; *S_d*, stemflow depth; SR, stemflow rate; FR, funneling ratio.

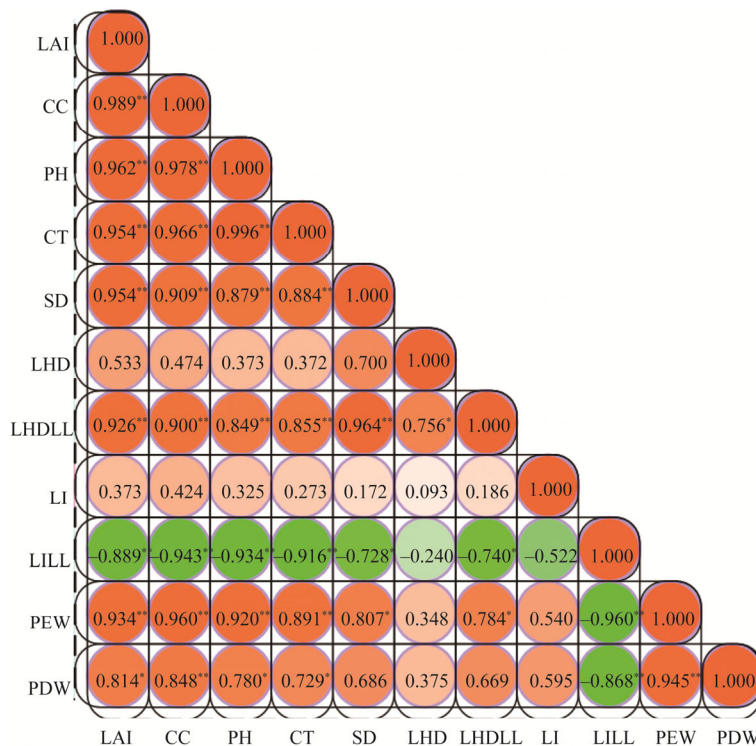


Fig. 7 Correlation among plant morphological parameters. *, $P<0.05$ level; **, $P<0.01$ level. The abbreviations are the same as in Table 2.

(excluding individual data; $R^2 < 0.80$, $P > 0.05$). The mechanism of droplet diameter on stemflow at different sprinkler intensities was not consistent due to the disturbance of sprinkler intensity and the limitation of maize leaf channeling capacity. Therefore, this study could not obtain the prediction model for stemflow depth and rate based on different droplet diameters. In addition, to verify the obtained model's predictive accuracy and application reliability, the remaining experimental data were used to compare and analyze the differences between measured and simulated values. As shown in Figure 8, the slopes of linear regressions between measured and simulated values were very close to 1.00, and the determination coefficients of regression equations were greater than 0.98. Also, the RMSE and NRMSE were at very low levels. In summary, the predictive models for stemflow depth and rate based on different sprinkler intensities were reliable and precise.

Table 3 Non-linear regression analysis between stemflow depth, rate and canopy closure

Sprinkler water physical feature	Stemflow depth and rate	Regression model	R^2	P	
Sprinkler intensity (mm/h)	10	$S_{d:10}$	$S_{d:10}=0.022\times CC^{1.09}$	0.84	<0.01
		SR_{10}	$SR_{10}=0.200\times CC^{1.11}$	0.92	<0.01
	20	$S_{d:20}$	$S_{d:20}=0.061\times CC^{1.08}$	0.95	<0.01
		SR_{10}	$SR_{10}=0.300\times CC^{1.08}$	0.94	<0.01
	30	$S_{d:30}$	$S_{d:30}=0.090\times CC^{1.10}$	0.96	<0.01
		SR_{30}	$SR_{30}=0.291\times CC^{1.10}$	0.94	<0.01
Droplet diameter (mm)	1.48	$S_{d:1.48}$	$S_{d:1.48}=0.071\times CC^{1.05}$	0.27	>0.05
		$SR_{1.48}$	$SR_{1.48}=0.335\times CC^{1.05}$	0.69	>0.05
	3.67	$S_{d:3.67}$	$S_{d:3.67}=0.109\times CC^{0.93}$	0.23	>0.05
		$SR_{3.67}$	$SR_{3.67}=0.335\times CC^{1.05}$	0.69	>0.05
	7.11	$S_{d:7.11}$	$S_{d:7.11}=0.048\times CC^{1.13}$	0.34	>0.05
		$SR_{7.11}$	$SR_{7.11}=0.226\times CC^{1.12}$	0.88	<0.01

Note: S_d , stemflow depth; SR, stemflow rate; CC, canopy closure.

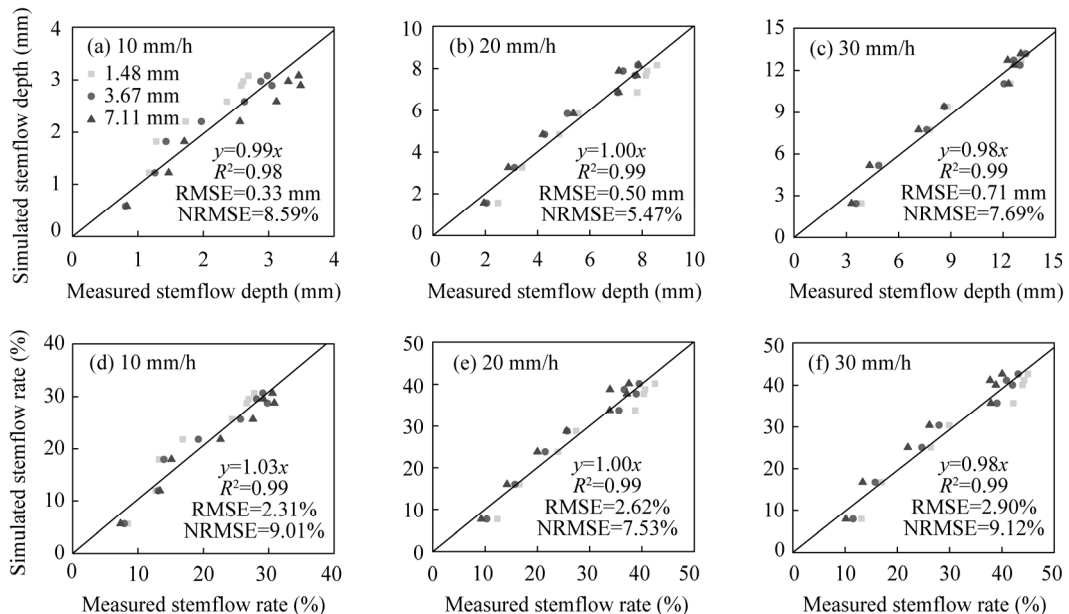


Fig. 8 Comparison between measured and predicted stemflow depth (a–c) and rate (d–f) at different sprinkler intensities. RMSE, root mean square error; NRMSE, standard root mean square error.

4 Discussion

4.1 Spatial-temporal variation of stemflow and its influence factors

From the pre-jointing stage to the late filling stage, the length, width, number, and inclination of leaves, plant height, canopy closure and structure of maize show a growing or thickening pattern (Panozzo et al., 2019). Moreover, maize resembles the shape of a funnel with an upward opening. If the number of leaves and leaf inclination are the greater, the maize plant's shape and funnel's catchment area are larger, and the ability of maize to produce stemflow would be greater (De Ploey, 1982; Van Elewijck, 1989). The present findings are consistent with previous studies. For example, Liu et al. (2015) found that as LAI increased from 1.00 to 4.50 m²/m², stemflow rate would increase from 10.00% to 40.00%. Their results also suggested that the ability of maize plant to funnel sprinkler water showed a positive linear correlation with leaf area per plant. Zheng et al. (2018) analyzed the correlation between maize stemflow and morphological parameters in the field, and their results showed that stemflow amount and rate increased with the growth of maize. Our results also revealed that stemflow rate increased from less than 10% to almost 40% as maize grew (Fig. 4). Additionally, using sprinkler irrigation as the test condition, Lamm and Manges (2000) obtained values of stemflow rates that agreed with the present study. However, as shown in Figure 4d, during the growing season in 2021, maize exhibited a higher funneling ratio at the jointing stage than at other growth stages, which was contrary to the initial hypothesis and previous studies. After analyzing the reason for this phenomenon, we found that the stem diameter at the jointing stage was smaller. Of course, similar findings were not only found for crop families but also for bananas (Cattan et al., 2007), scrubs (Yang et al., 2018; Zhang et al., 2020), and forest trees (Yang et al., 2018), which the effects of morphological parameters on stemflow amount, rate, and funneling ratio were found to be nearly consistent. Fan et al. (2015) revealed that stemflow amount of large pines was 2.5 times higher than that of small-sized ones. Moreover, Zhang et al. (2020) found that if the shape size of shrubs was larger, stemflow amount would be greater. The plant's number of leaves, basal area, and canopy projection area positively affected stemflow amount, rate, and funneling ratio. Therefore, the changes in stemflow generation throughout the growing season were highly consistent with the variation of plant morphological parameters, i.e., the variation of morphological parameters resulted in significant differences in funneling sprinkler water.

The whole maize plant could be regarded as a multi-layered canopy structure from top to bottom. The present results showed that the ability of upper canopy to generate stemflow decreased gradually as maize plant grew from the jointing to the flare opening stage, while the reverse was true for the lower canopy. From the tasseling stage to the filling stage, the ability of middle canopy to produce stemflow increased, while the upper and lower canopies decreased (Fig. 5). Zapata et al. (2021) analyzed how the maize leaves at different positions influenced the kinetic energy of sprinkler water droplets. Their results were similar to the present study. They also found that maize leaves at the middle canopy (around 1.50 m above the ground) significantly dissipated the kinetic energy. We monitored the spatiotemporal variations in the morphological parameters of maize canopies at different positions. As shown in Table 4, leaf length, width, effective surface area, leaf height distance, leaf inclination, and biomass for the upper canopy were significantly greater than the lower canopy at the jointing stage. We found that the variation in morphological parameters described above was the primary driver for the greater amount of stemflow generated by the upper canopy. In addition, the shape of mature maize plant is not pyramidal but elliptical, i.e., small at both ends and large in the middle (Wang et al., 2020; Wu et al., 2021). The leaves on the stem are spirally distributed. If there were a positive value for the lower canopy closure, then it would suggest that the canopy at that position was also directly exposed to sprinkler water or rainfall. Combining Figure 5 and Table 4, we found that the ability of maize canopy at different spatial positions and growth stages to funnel sprinkler water was more consistent with the corresponding canopy closure rather than other parameters, i.e., the ability to generate stemflow

Table 4 Plant morphological parameters at different spatial positions and growth stages

Growth stage	Canopy layer	Morphological parameters									
		LL (cm)	LW (cm)	LN	ESA (cm ²)	CT (cm)	CC (%)	LHD (cm)	LI (°)	LCFW (g)	LCDW (g)
		2020									
JS	Whole	70.81±9.48	6.93±2.12	8	2944.40±642.15	89.95±11.36	39.84	26.13±7.16	69.53±17.46	72.30±15.17	10.12±2.13
	Upper	72.92±13.18	8.16±1.02	4	1785.12±701.31	54.48±9.02	28.79	29.85±5.59	75.39±11.32	48.63±9.03	6.89±1.12
	Lower	67.56±7.16	5.72±1.06	4	1159.28±369.48	35.47±7.48	11.05	22.41±4.57	64.07±6.59	23.67±5.48	3.23±0.88
FOS	Whole	73.32±13.48	8.99±2.43	12	5932.66±994.12	214.18±31.26	68.47	21.53±6.78	69.21±13.26	227.61±46.51	34.14±6.14
	Upper	83.48±9.43	9.97±1.48	6	3745.17±549.63	136.65±26.49	49.51	17.59±6.45	74.18±11.26	143.57±31.21	22.13±5.41
	Lower	70.66±8.12	6.88±1.03	6	2187.49±501.12	77.53±11.02	18.96	25.47±9.48	64.24±9.38	84.04±11.05	12.01±3.16
TS	Whole	82.33±15.48	9.46±3.47	14	8333.14±2997.62	224.45±29.68	87.96	21.88±6.49	72.38±13.36	559.96±162.15	136.18±14.97
	Upper	61.81±5.91	8.45±1.26	5	1958.67±348.69	83.45±11.26	26.14	13.92±4.59	82.16±12.24	69.15±8.49	12.01±1.99
	Middle	97.50±16.48	10.59±2.01	5	4027.29±1548.13	93.12±12.69	78.16	34.18±8.49	70.06±8.46	435.18±29.48	110.48±13.25
FS	Lower	82.97±7.11	9.43±1.98	4	2347.18±536.15	47.88±8.46	9.80	17.54±6.47	65.32±8.49	55.63±11.48	13.69±3.52
	Whole	74.83±9.69	9.98±3.47	15	8659.74±2496.51	234.12±27.18	93.18	23.69±6.98	71.58±18.57	1110.14±236.47	428.02±35.68
	Upper	62.15±8.51	8.15±2.12	5	1899.47±249.68	88.69±12.25	29.69	13.11±2.38	83.46±12.46	83.48±13.48	14.67±2.98
	Middle	95.16±16.47	10.95±2.59	5	4165.59±1689.48	97.25±19.68	86.47	38.48±9.57	67.10±11.41	962.07±148.59	399.36±37.57
	Lower	76.62±11.34	9.03±1.87	5	2594.68±697.49	48.18±7.13	6.71	19.48±7.62	64.58±10.15	64.59±12.36	13.99±4.51
	2021										
JS	Whole	38.10±8.48	6.11±2.37	6	1047.61±258.37	52.00±11.24	20.15	16.86±8.49	71.43±16.67	23.88±5.14	4.34±1.02
	Upper	38.51±9.62	7.48±2.11	3	648.15±691.15	30.62±6.57	13.11	19.75±8.14	74.21±12.32	14.62±4.95	2.59±1.05
	Lower	29.64±5.68	5.99±1.59	3	399.46±43.65	21.38±4.02	7.04	13.97±5.69	69.05±13.26	9.26±3.11	1.75±0.63
FOS	Whole	81.53±15.24	8.57±3.42	10	5240.63±1694.25	163.11±19.12	57.46	23.17±7.48	71.50±12.35	164.44±16.69	24.67±5.49
	Upper	87.19±8.49	9.11±2.11	5	2978.60±659.48	91.18±8.59	39.87	20.16±6.98	77.58±10.29	89.47±10.39	14.08±3.26
	Lower	78.15±8.16	8.02±1.58	5	2262.03±489.36	71.93±5.98	17.59	26.18±10.42	65.42±6.95	74.97±8.59	10.59±2.49
TS	Whole	85.51±16.25	9.19±3.59	12	7072.73±2456.18	217.03±16.98	79.32	22.27±4.97	70.40±12.51	201.45±23.65	34.25±4.68
	Upper	71.93±8.14	9.03±1.39	4	1948.52±397.17	76.48±12.69	28.29	14.58±5.41	75.54±9.19	50.16±10.59	7.95±2.01
	Middle	90.17±13.49	10.59±2.14	4	2864.85±419.78	85.69±16.95	69.85	32.12±7.49	74.08±10.26	91.23±20.47	17.81±2.98
FS	Lower	84.72±10.34	8.89±1.49	4	2259.36±349.95	54.86±7.48	9.47	20.11±5.98	61.58±9.21	60.06±9.48	8.49±1.25
	Whole	86.61±16.94	9.84±3.15	14	8035.03±1943.51	221.84±15.68	90.18	26.19±8.19	73.13±13.24	704.45±199.47	252.96±36.57
	Upper	75.46±9.48	9.01±2.16	5	2549.68±599.47	78.57±9.49	21.41	16.53±5.17	80.26±11.02	68.48±16.52	12.48±2.95
	Middle	97.90±11.29	11.96±1.97	5	3340.23±497.21	90.59±8.95	84.11	41.86±19.57	79.26±14.39	569.38±149.56	227.46±59.61
	Lower	86.47±8.48	9.35±2.03	4	2145.12±336.49	52.68±6.49	6.07	20.18±6.48	59.47±9.87	66.59±13.65	13.02±3.01

Note: JS, jointing stage; FOS, flare opening stage; TS, tasseling stage; FS, filling stage. LL, leaf length; LW, leaf width; LN, number of leaves; ESA, effective surface area; CT, canopy thickness; CC, canopy closure; LHD, leaf-height distance; LI, leaf inclination; LCFW, leaf and cob fresh weight; LCDW, leaf and cob dry weight. Mean±SD.

would increase with canopy closure. In other words, when the maize canopy was divided into several parts, the parameter that characterized the ability to generate stemflow at different positions was canopy closure rather than other morphological parameters.

4.2 Effects of sprinkler characteristics on stemflow

The increase or decrease of sprinkler intensity indicates not only the change in water volume per unit area per unit time but also the kinetic energy of water droplet population striking the plant leaves (Table 1). As sprinkler intensity increased, the more sprinkler water would fall on the leaves' surface, and the more stemflow would be collected and generated by the plant canopy. If the canopy catchment area was a specific value, then certainly the stemflow (stemflow amount and depth) collected and generated by the plants would increase with increasing sprinkler intensity. Namely, by increasing sprinkler intensity, stemflow amount and depth would naturally increase (Fig. 6a–d). Similar conclusions were also obtained from previous studies on stemflow yielded by crop canopies (Lamm and Manges, 2000; Zheng et al., 2018, 2019), woods (Park and Hattori, 2002; Fan et al., 2015; Zabret et al., 2018; Tonello et al., 2021), and shrubs (Zhang et al., 2015, 2016; Yang et al., 2018). However, some findings significantly differed from present study. They concluded that sprinkler irrigation or rainfall intensity negatively correlated with indicators characterizing the ability to generate stemflow (Ma et al., 2008a; Liu et al., 2015). On the one hand, they believed that when plant leaves or branches conveyed stemflow, stemflow produced with larger sprinkler or rainfall water amount exceeded the transport capacity of the available pathways, resulting in overloading of the transport channels and forcing part of stemflow to gradually convert to throughfall (Crockford and Richardson, 2015). On the other hand, larger kinetic energy represented greater impacting forces. Compared with smaller kinetic energy, plant leaves would be significantly shaken and misshapen when a certain magnitude or level of kinetic energy impacted the leaves. The pre-existing shape or form of leaves might then be disrupted, ultimately resulting in changes to the current catchment area of canopy or leaves (Zheng et al., 2019). We set the installation height of needles to a constant 0.50 m above maize canopy. Although the increase in sprinkler intensity was large, the droplet falling height remained within a relatively small range. The kinetic energy was related to the water amount, the droplet velocity and size (Frasson and Krajewski, 2011), and the higher falling distance corresponded to the larger droplet landing velocity (Wang and Pruppacher, 1976). The present findings showed no significant increase in stemflow rate or funneling ratio despite the large increase in sprinkler intensity. We considered that the kinetic energy of higher sprinkler intensity in this study did not significantly change the water catchment area of maize canopy or leaves, and that the stemflow generated at this time did not completely clog the transport pathways.

It was worth mentioning that the effect of droplet size on generating stemflow was initially clarified in this study. Our results indicated that droplet diameter significantly affected stemflow generating, i.e., the larger the droplet size, the smaller the stemflow generation (Fig. 6). The motion of sprinkler water droplets on maize leaves consists of convergence, retention, breaking, and splashing (Frasson and Krajewski, 2011). Moreover, the motion of different droplet sizes on maize leaves varies enormously (Dorr et al., 2015). We observed that droplet size affected the run-off path of stemflow on maize leaves, and a schematic representation of these effects was used to illustrate the process. Under the small droplet diameter of 1.48 mm, the smaller droplets' impact on the stemflow flowing paths was negligible (Fig. 9a). However, as shown in Figure 9b and c, remarkable break-up occurred when the water droplets with diameters of 3.67 and 7.11 mm. The instantaneous breaking of larger droplets acted as a 'barrage' dam blocking the stemflow paths, resulting in the overflow of stemflow in the upper stream, thus converting part of the stemflow into throughfall. This phenomenon appeared significantly with increasing droplet size (Fig. 9c). Additionally, we found an amusing phenomenon. As shown in Figure 6a–h, when the sprinkler intensity was 10 mm/h, the stemflow amount, depth, rate, and funneling ratio increased significantly with increasing droplet diameter. Only when the sprinkler intensity was greater

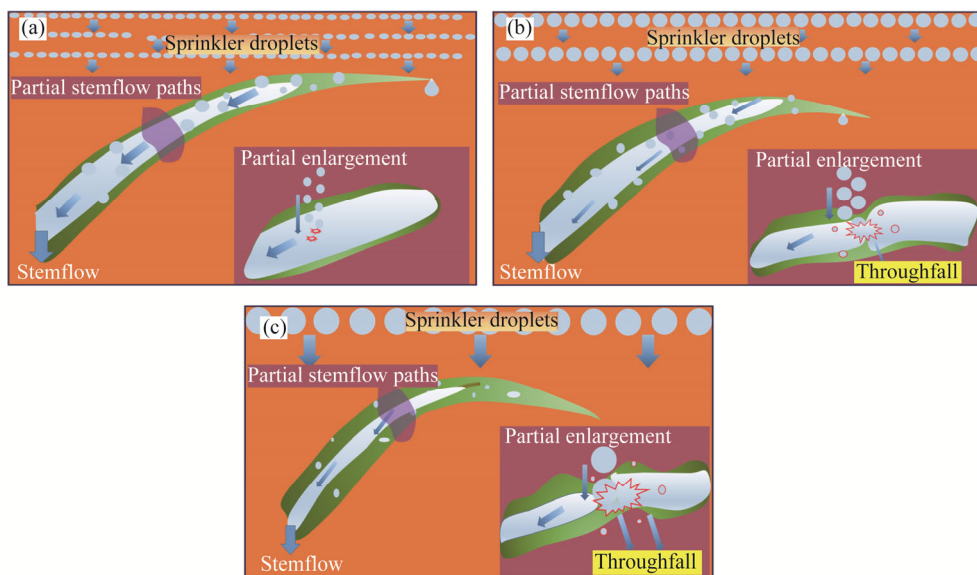


Fig. 9 Schematic diagram of the effect of droplets with different sizes on stemflow channels on maize leaves. (a), small diameter water droplets; (b), medium diameter water droplets; (c), large diameter water droplets.

than or equal to 20 mm/h did the four stemflow parameters decrease with increasing the droplet size. The above results showed that the process by which droplet size affected the plant stemflow changed considerably when the sprinkler intensity varied. The kinetic energy, swings, and deformation of maize leaves were small when the sprinkler intensity was 10 mm/h (Table 1). At this point, the width of pathway conveying stemflow was such that even larger water droplets striking the pathway did not cause a complete cut-off. What's more, when the sprinkler intensity was a particular value, the larger droplet group corresponded to a smaller droplet density, at which time the larger droplets had a greater chance of being converted to stemflow.

4.3 Correlation between morphological parameters and stemflow

The current results indicated that as plant morphological parameters increased, the stemflow amount, depth, and rate increased significantly (Table 2). Similar positive correlations between stemflow and plant morphological parameters have been obtained in previous studies. Ma et al. (2008b) showed that stemflow rate increased as a power function with increasing LAI of maize plant. When LAI increased from the minimum to the maximum value, the corresponding stemflow rate increased from 5% to 70%. Zheng et al. (2019) found a positive correlation between stemflow and canopy closure. In addition, Levia and Germer (2015) reviewed the effect of wood canopy structure on stemflow generation, and concluded a positive correlation between stemflow and plant morphological parameters. However, different field management patterns and crop varieties resulted in large differences between plant morphological parameters (Germer et al., 2010). Several researchers have found that plant morphological parameters negatively affected stemflow (Germer et al., 2010; Wang et al., 2013). Therefore, we should carry out more research on the ability of plants to generate stemflow in the future.

In addition, the prediction model for stemflow developed by previous researchers has used the leaf height distance and leaf inclination as two important morphological parameters (De Ploey, 1982; Van Elewijck, 1989). However, the present results revealed that leaf height distance and leaf inclination only showed weak positive correlations with stemflow amount, depth, and rate ($0.30 < R^2 < 0.50$, $P > 0.05$; Table 2). The shape of maize plant resembles an ellipsoid (large in the middle and small at the ends). If average method was used to calculate these two parameters, it would weaken the contribution of middle canopy to stemflow generation. In this light, we measured the leaf height distance and leaf inclination of larger leaves. The results showed that leaf height distance and leaf inclination of larger leaves were significantly correlated with

stemflow amount, depth, and rate ($R^2 > 0.80$, $P < 0.01$; Table 2). The findings indicated that the leaf height distance and inclination of larger leaves contributed more to stemflow generation. However, the leaf inclination is an angle between main vein and horizontal plane, and if the leaf inclination is very small or close to zero, we have to question the stemflow fluidity on leaves. Therefore, the mechanism of effect of leaf inclination on stemflow will require further study.

Furthermore, the results of funneling ratio were contrary to previous research (Liu et al., 2015; Yang et al., 2018). Funneling ratio characterizes the ability of whole maize plant to generate stemflow, and it may not be realistic to use a particular morphological parameter to characterize its value. In addition, this study was carried out on a community rather than a single maize plant, and there was a degree of shading between maize leaves at different orientations on the micro-scale spatial scope.

4.4 Research prospects

Compared with sprinkler head with a given spraying angle, water droplets of this study landed almost vertically on the maize canopy. Such an experimental design might affect the applied value of research findings. Although our findings showed that variations in droplet landing angle could affect the probability of droplets' contact with maize leaves or canopy, it was not clear whether droplet landing angle could significantly affect stemflow generation. To comprehensively understand the mechanism by which the sprinkler droplet physical parameters affect crop canopy to generate stemflow, the sprinkler droplet landing angle will be one of directions for future research. In addition, regression tree analysis can reasonably evaluate the contribution of numerous factors to stemflow generation in plant canopy. Moreover, up to now, many scholars have used this method to analyze the main controlling factors influencing stemflow generated by forest canopy. However, the method has not yet been applied to sprinkler irrigation and crops.

5 Conclusions

In this study, the plant's ability to generate stemflow increased with the growth of maize plant, and reached the maximum at the filling stage. At the jointing and flare opening stages, the upper canopy produced more stemflow than the lower canopy. The middle canopy was significantly more capable of generating stemflow than other positions of canopy at the tasseling and filling stages. Canopy closure was the main factor contributing to the differences in the canopy's ability at different positions to generate stemflow. Stemflow increased with increasing sprinkler intensity. However, the mechanism by which droplet size with different sprinkler intensities affected stemflow generation was not consistent. When sprinkler intensity was less than or equal to 10 mm/h, stemflow generation increased as the droplet diameter increased. However, if sprinkler intensity was greater than or equal to 20 mm/h, stemflow generation was reverse. The effect of canopy closure on stemflow amount, depth, and rate was more noticeable than other morphological parameters, and canopy closure could well characterize the morphology of four maize plants at the micro-scale spatial scope. We have only developed regression models for stemflow depth versus canopy closure, and stemflow rate versus canopy closure with a high predictive accuracy based on different sprinkler intensities. The mechanism by which droplet size affects the plant's ability to funnel sprinkler water or rainfall should still be the focus of our future research.

Acknowledgements

This study was funded by the National Natural Science Foundation of China (52009111), the National Key Research and Development Program of China (2021YFE010300), and the Key Research and Development Program of Shaanxi Province, China (2020ZDLNY01-01).

References

Carlyle-Moses D E, Iida S, Germer S, et al. 2018. Expressing stemflow commensurate with its ecohydrological importance.

- Advances in Water Resources, 121: 472–479.
- Cattan P, Bussiere F, Nouvellon A. 2007. Evidence of large rainfall partitioning patterns by banana and impact on surface runoff generation. *Hydrological Processes*, 21(16): 2196–2205.
- Chen N, Zhang Y, Zhao C. 2021. On the importance of stemflow to the woody plants in drylands: Individual vs. ecosystem scales. *Journal of Hydrology*, 601: 126591, doi: 10.1016/j.jhydrol.2021.126591.
- Chen R, Li H, Wang J, et al. 2020. Effects of pressure and nozzle size on the spray characteristics of low-pressure rotating sprinklers. *Water*, 12(10): 2904, doi: 10.3390/w12102904.
- Crockford R H, Richardson D P. 2015. Partitioning of rainfall into throughfall, stemflow and interception: effect of forest type, ground cover and climate. *Hydrological Processes*, 14(1617): 2903–2920.
- De Ploey J. 1982. A stemflow equation for grasses and similar vegetation. *CATENA*, 9(1): 139–152.
- Dorr G J, Wang S, Mayo L C, et al. 2015. Impaction of spray droplets on leaves: influence of formulation and leaf character on shatter, bounce and adhesion. *Experiments in Fluids*, 56(7): 1–17.
- Fan J L, Oestergaard K T, Guyot A, et al. 2015. Spatial variability of throughfall and stemflow in an exotic pine plantation of subtropical coastal Australia. *Hydrological Processes*, 29(5): 793–804.
- Frasson R P D M, Krajewski W F. 2011. Characterization of the drop-size distribution and velocity–diameter relation of the throughfall under the maize canopy. *Agricultural and Forest Meteorology*, 151(9): 1244–1251.
- Ge M S, Wu P T, Zhu D L, et al. 2018. Analysis of kinetic energy distribution of big gun sprinkler applied to continuous moving hose-drawn traveler. *Agricultural Water Management*, 201: 118–132.
- Germer S, Werther L, Elsenbeer H. 2010. Have we underestimated stemflow? Lessons from an open tropical rainforest. *Journal of Hydrology*, 395(3–4): 169–179.
- Glover J, Gwynne M D. 1962. Light rainfall and plant survival in east Africa. I. Maize. *Journal of Ecology*, 50: 111–118.
- Herwitz S R. 1986. Infiltration-excess caused by Stemflow in a cyclone-prone tropical rainforest. *Earth Surface Processes and Landforms*, 11(4): 401–412.
- Hou P, Liu Y E, Liu W M, et al. 2021. Quantifying maize grain yield losses caused by climate change based on extensive field data across China. *Resources, Conservation and Recycling*. 174: 105811, doi: 10.1016/j.resconrec.2021.105811.
- Kang Y H, Wang Q G, Liu H J. 2005. Winter wheat canopy interception and its influence factors under sprinkler irrigation. *Agricultural Water Management*, 74(3): 189–199.
- Lamm F R, Manges H L. 2000. Partitioning of sprinkler irrigation water by a corn canopy. *Transactions of the ASABE*, 43(4): 909–918.
- Levia D F, Frost E E. 2003. A review and evaluation of stemflow literature in the hydrologic and biogeochemical cycles of forested and agricultural ecosystems. *Journal of Hydrology*, 274(1–4): 1–29.
- Levia D F, Germer S. 2015. A review of stemflow generation dynamics and stemflow–environment interactions in forests and shrublands. *Reviews of Geophysics*, 53(3): 673–714.
- Levia D F, Hudson S A, Llorens P, et al. 2017. Throughfall drop size distributions: a review and prospectus for future research. *Wiley Interdisciplinary Reviews: Water*, 4(4): e1225, doi: 10.1002/wat2.1225.
- Li X, Xiao Q F, Niu J Z, et al. 2016. Process-based rainfall interception by small trees in Northern China: The effect of rainfall traits and crown structure characteristics. *Agricultural and Forest Meteorology*, 218–219: 65–73.
- Liu H J, Zhang R H, Zhang L W, et al. 2015. Stemflow of water on maize and its influencing factors. *Agricultural Water Management*, 158: 35–41.
- Ma B, Wu F Q, Ma F, et al. 2008. Effect of leaf area and rainfall intensity on the stemflow of Glycine max. *Science of Soil and Water Conservation*, 6(6): 58–62. (in Chinese)
- Ma F, Wu F Q, Ma B, et al. 2008. Effects of leaf area and rainfall intensity on stemflow amount through corn canopy. *Transactions of the CSAE*, 24(10): 25–28. (in Chinese)
- Neave M, Abrahams A D. 2002. Vegetation influences on water yields from grassland and shrubland ecosystems in the Chihuahuan Desert. *Earth Surface Processes and Landforms*, 27(9): 1011–1020.
- Panozzo A, Cortivo C D, Ferrari M, et al. 2019. Morphological changes and expressions of AOX1A, CYP81D8, and putative PFP genes in a large set of commercial maize hybrids under extreme waterlogging. *Frontiers in Plant Science*, 10(62): 1–14.
- Park H T, Hattori S. 2002. Applicability of stand structural characteristics to stemflow modeling. *Journal of Forest Research*, 7(2): 91–98.
- Patrignani A, Ochsner T E. 2015. Canopeo: a powerful new tool for measuring fractional green canopy cover. *Agronomy Journal*, 107(6): 2312–2320.

- Saffigna P G, Tanner C B, Keeney D R. 1976. Non-uniform infiltration under potato canopies caused by interception, stemflow, and hilling. *Agronomy Journal*, 68(2): 337–342.
- Sher A, Khan A, Ashraf U, et al. 2018. Characterization of the effect of increased plant density on canopy morphology and stalk lodging risk. *Frontiers in Plant Science*, 9: 1047, doi: 10.3389/fpls.2018.01047.
- Taniguchi M, Tsujimura M, Tanaka T. 2015. Significance of stemflow in groundwater recharge. I: Evaluation of the stemflow contribution to recharge using a mass balance approach. *Hydrological Processes*, 10(1): 71–80.
- Tonello K C, Van Stan II J T, Rosa A G, et al. 2021. Stemflow variability across tree stem and canopy traits in the Brazilian Cerrado. *Agricultural and Forest Meteorology*, 308–309: 108551, doi: 10.1016/j.agrformet.2021.108551.
- Van Elewijck L L. 1989. Stemflow on maize: A stemflow equation and the influence of rainfall intensity on stemflow amount. *Soil Technology*, 2(1): 41–48.
- Waiters R J, Price A G. 1988. The influence of stemflow from standing dead trees on the fluxes of some ions in a mixed deciduous forest. *Canadian Journal of Forest Research*, 18(11): 1490–1493.
- Walczak A. 2021. The use of world water resources in the irrigation of field cultivations. *Journal of Ecological Engineering*, 22(4): 186–206.
- Wang P K, Pruppacher H R. 1976. Acceleration to terminal velocity of cloud and raindrops. *Journal of Applied Meteorology*, 16(3): 275–280.
- Wang X P, Zhang Y F, Wang Z N, et al. 2013. Influence of shrub canopy morphology and rainfall characteristics on stemflow within a vegetated sand dune in the Tengger Desert, N&W China. *Hydrological Processes*, 27(10): 1501–1509.
- Wang Y L, Li M N, Hui X, et al. 2020. Alfalfa canopy water interception under low-pressure sprinklers. *Agricultural Water Management*, 230: 105919, doi:10.1016/j.agwat.2019.105919.
- Whitford W G, Anderson J, Rice P M. 1997. Stemflow contribution to the 'fertile island' effect in Creosote bush, *Larrea tridentata*. *Journal of Arid Environments*, 35(3): 451–457.
- Wu D F. 1987. Sprinkler intensity and soil infiltration. *Water Saving Irrigation*, (2): 15–20. (in Chinese)
- Wu Y S, He D, Wang E L, et al. 2021. Modelling soybean and maize growth and grain yield in strip intercropping systems with different row configurations. *Field Crops Research*, 265: 108122, doi: 10.1016/j.fcr.2021.108122.
- Yang J M, Yang J Y, Liu S, et al. 2014. An evaluation of the statistical methods for testing the performance of crop models with observed data. *Agricultural Systems*, 127(5): 81–89.
- Yang X L, Shao M A, Wei X R. 2018. Stemflow production differ significantly among tree and shrub species on the Chinese Loess Plateau. *Journal of Hydrology*, 568: 427–436.
- Yin X A, Fang Q, Yang T H, et al. 2020. Effect of simulated corn stemflow on soil erosion. *Journal of Soil and Water Conservation*, 34(3): 67–72. (in Chinese)
- Zabret, Rakovec, Sraj. 2018. Influence of meteorological variables on rainfall partitioning for deciduous and coniferous tree species in urban area. *Journal of Hydrology*, 558: 29–41.
- Zapata N, Robles O, Playán E, et al. 2018. Low-pressure sprinkler irrigation in maize: Differences in water distribution above and below the crop canopy. *Agricultural Water Management*, 203: 353–365.
- Zapata N, Salvador R, Latorre B, et al. 2021. Effect of a growing maize canopy on solid-set sprinkler irrigation: kinetic energy dissipation and water partitioning. *Irrigation Science*, (39): 329–346.
- Zhang Y F, Wang X P, Hu R, et al. 2015. Rainfall partitioning into throughfall, stemflow, and interception loss by two xerophytic shrubs within a rain-fed revegetated desert ecosystem, northwestern China. *Journal of Hydrology*, 527: 1084–1095.
- Zhang Y F, Wang X P, Hu R, et al. 2016. Throughfall and its spatial variability beneath xerophytic shrub canopies within water-limited arid desert ecosystems. *Journal of Hydrology*, 539: 406–416.
- Zhang Y F, Wang X P, Pan Y X, et al. 2020. Relative contribution of biotic and abiotic factors to stemflow production and funneling efficiency: A long-term field study on a xerophytic shrub species in Tengger Desert of northern China. *Agricultural and Forest Meteorology*, 280: 107781, doi:10.1016/j.agrformet.2019.107781.
- Zhang Y S, Zhu D L. 2017. Influence of sprinkler irrigation droplet diameter, application intensity and specific power on flower damage. *Frontiers of Agricultural Science and Engineering*, 4(2): 165–171.
- Zhao W X, Zhang M, Li J S, et al. 2018. Influence of sprinkler height on irrigation performance of center pivot irrigator. *Transactions of the Chinese Society of Agricultural Engineering*, 34(10): 107–112. (in Chinese)
- Zheng J, Fan J L, Zhang F C, et al. 2018. Rainfall partitioning into throughfall, stemflow and interception loss by maize canopy on the semi-arid Loess Plateau of China. *Agricultural Water Management*, 195: 25–36.

- Zheng J, Fan J L, Zhang F C, et al. 2019. Throughfall and stemflow heterogeneity under the maize canopy and its effect on soil water distribution at the row scale. *Science of the Total Environment*, 660(10): 1367–1382.
- Zhu Z R, Zhu D L, Ge M S. 2021. The spatial variation mechanism of size, velocity, and the landing angle of throughfall droplets under maize canopy. *Water*, 13(15): 2083, doi: 10.3390/w13152083.
- Zhu Z R, Zhu D L, Ge M S. 2022. Drop size distribution and effective determination of the constitution of throughfall droplets under maize canopy. *CLEAN-Soil Air Water*, 50(5): 20210280, doi: 10.1002/clen.202100280.
- Zul Hilmi Saidin A, Delphis F, Levia B C, et al. 2022. Vertical distribution and transport of radiocesium via branchflow and stemflow through the canopy of cedar and oak stands in the aftermath of the Fukushima Dai-ichi Nuclear Power Plant accident. *Science of the Total Environment*, 125: 151698, doi:10.1016/j.scitotenv.2021.151698.

Fig. S1 Basic structure of sprinkler unit (a) and needle spraying method (b)

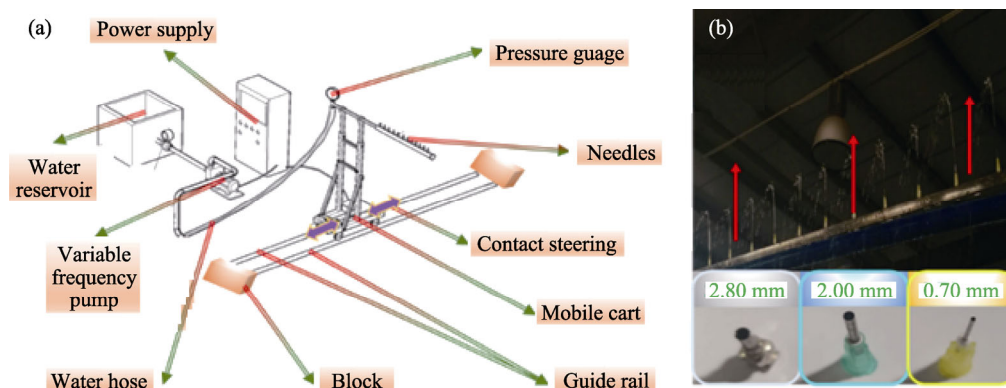


Fig. S2 Adjustment of sprinkler water droplet diameter and needle installation height

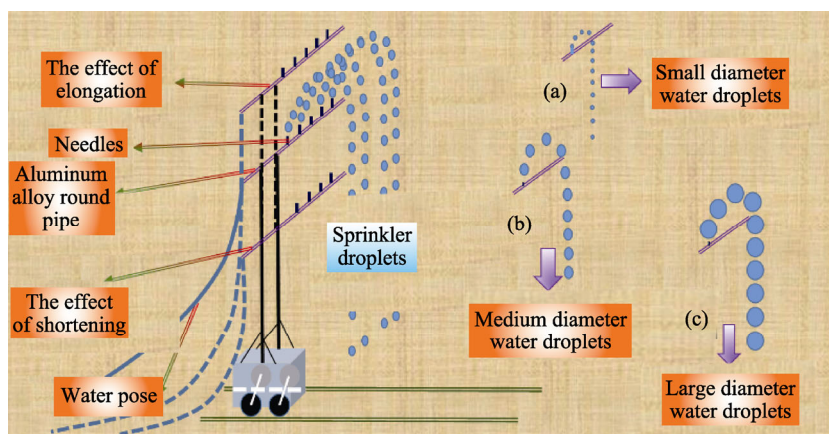


Fig. S2 Adjustment of sprinkler water droplet diameter and needle installation height

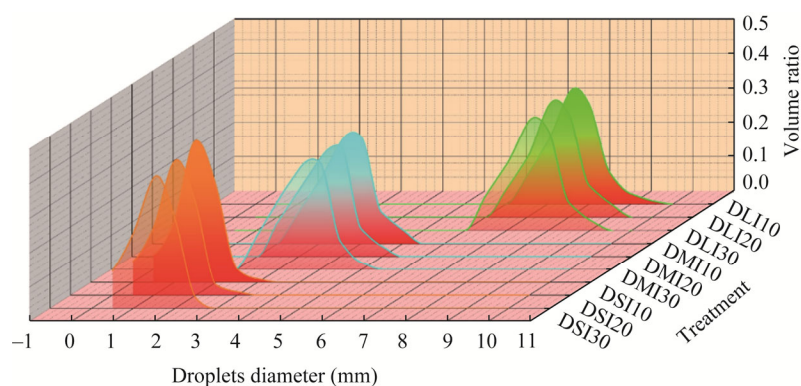


Fig. S3 Drop size distribution among different treatments. Red filling represented the small diameter water droplets; cyan filling represented the medium diameter water droplets; yellow-green filling represented the large diameter water droplets. Less transparent filling represented the lighter sprinkler intensity. The detailed treatments can be found in Table 1.

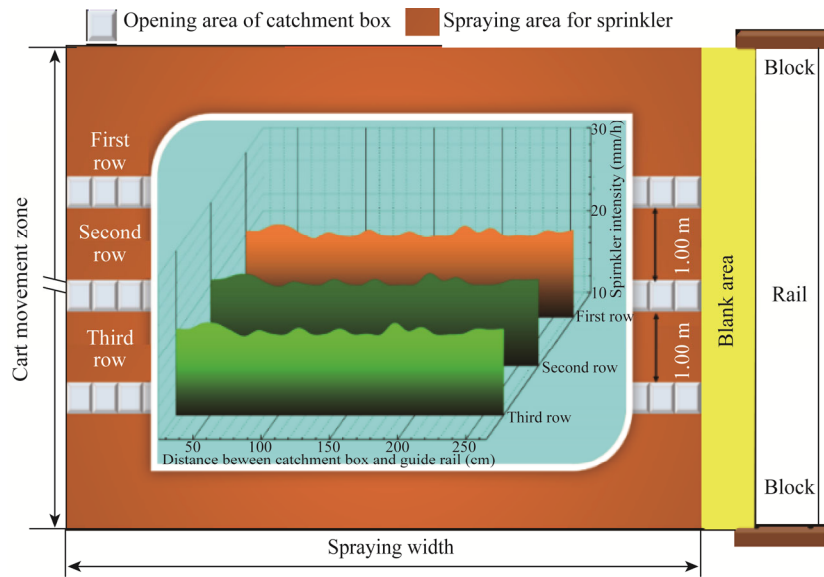


Fig. S4 Spatial distribution of sprinkler water